A mass-limited Sn target irradiated by dual laser pulses for an EUVL source

Y.Tao[*1, 2], M.S.Tillack[1, 2], K.L.Sequoia[1, 2], and F.Najmabadi[2, 3]
[1]Department of Mechanical and Aerospace Engineering,
[2]Center for Energy Research,
[3]Department of Electrical and Computer Engineering,
University of California, San Diego. 9500 Gilman Drive, La Jolla, CA, USA 92093-0417

ABSTRACT

We present efforts to mitigate debris from laser-produced Sn plasma by introducing a low energy pre-pulse while keeping high in-band conversion efficiency from laser to 13.5 nm extreme ultraviolet (EUV) light. The basic idea is to separate the processes of plasma production and 13.5 nm EUV light generation. A low energy pre-pulse is introduced to create a pre-plume; the main pulse then heats up the pre-plume to the optimum temperature for efficient 13.5 nm EUV light generation. Much lower ion energy and nearly the same conversion efficiency were simultaneously observed from plasma driven by a dual-pulse as compared with that of a single pulse. Thin Sn coating were investigated as a form of mass-limited target. It was found that the higher ion energy normally accompanying the use of a mass-limited Sn target is effectively maintained under 100 eV by using the dual pulse irradiation technique. A Sn coating as thin as 30 nm could generate almost the same conversion efficiency as that obtained with a single pulse and a massive target. It was noted that less gas is required to mitigate ions with lower energy when dual pulses are used. This research enables an efficient, clean, and high-speed mass-limited target supply based on pure Sn for a high volume manufacturing (HVM) EUVL source.

Keywords: mass-limited, Sn, dual laser pulses, EUVL

1. INTRODUCTION

Extreme ultraviolet lithography is the most promising candidate for the next generation lithography tools used in the semiconductor industry to manufacture microchips with feature size of 32 nm or smaller [1]. However, several challenges in the development of EUVL have significantly delayed its commercial introduction. The number one challenge is to develop a powerful, clean, long lifetime, and stable EUV light source [2]. Most development efforts focus on in-band (2 % bandwidth) centered at 13.5 nm because of the availability of multilayer mirrors used in an EUVL system. In-band EUV power 115 to 180 W is required for high volume manufacturing (HVM); more power may be needed as system requirements evolve. Two main candidates for an EUVL light source are hot plasmas heated by electric discharge and high power pulsed laser [3, 4]. Even though at present discharge-pumped plasma can produce higher EUV power as compared with that of laser-produced plasma, and has been selected as the driver in alpha tools, the ability to scale to higher power makes LPP more promising as the driver in a practical EUVL system. Sn has been considered as the main fuel for an EUVL light source for its spectral peak located at 13.5 nm[5]. With the help of deeper understanding of the plasma physics of laser produced Sn plasmas [6, 7, 8], great progress has been achieved to enhance the in-band conversion efficiency from laser to 13.5 nm EUV light [9, 10, 11]. Further increases CE are possible by optimizing the parameters of the driving laser and target. However, debris remains an issue for laser produced Sn-based plasmas.

Because dense Sn plasma is optically thick to 13.5 nm EUV light [12], the in-band CE is determined by a trade-off between generation and re-absorption of 13.5 nm EUV light induced by the plasma itself [13,14]. In this spirit, using targets with a lower concentration of Sn atoms, high CE and less debris from Sn may be obtained simultaneously. Water droplets, liquid jets, low-density SnO_2, and low-density foam doped with Sn were investigated by several groups [15,16,17,18]. It has been shown that low-density foam doped with as low as 0.5 % concentration of solid density Sn could produce almost the same in-band CE from laser to 13.5 nm EUV light as compared with that of solid density Sn target [18]. But these low

* yetao@ucsd.edu; phone 1 858-534-7828; fax 1 858-822-2120

Emerging Lithographic Technologies XI, edited by Michael J. Lercel,
Proc. of SPIE Vol. 6517, 65173Q, (2007) · 0277-786X/07/$18
doi: 10.1117/12.725806

concentration targets are accompanied by extra ions with very fast velocity, such as C, O, and H, which are also critical to collector optics in EUVL.

High in-band CE has been obtained using pure Sn micro droplets and liquid jets, which are promising candidates as a target supply for EUVL sources based on laser-produced plasmas [19,20]. However, the large amount of debris due to the excess mass requires additional innovation. A thin Sn film with a thickness of 40 nm produces a similar in-band CE and much less neutral Sn emissions as compared with a massive Sn target [21,22]. Unfortunately, ions with high kinetic energy of several 10 keV were observed with a thin film target. The reason arises from the limited mass involved in the case of a thin film target [21]. Most of the atoms are ionized to high charge state. So more energy is gained during the plasma expansion. In this sense, higher ion energy always accompanies mass-limited targets. But the lifetime of the EUV optics strongly depends on ion energy, reduction in ion energy is necessary to extend the lifetime of the optics [23]. At the same time, slow ions are easy to stop with a gas, which is standard debris mitigation method used in EUVL and other soft and hard x-ray sources.

It is well known that ion acceleration in laser-produced plasma arises from plasma expansion [24]. The properties of the plasma expansion strongly depend on the initial plasma density profile. It has been pointed out that ion energy from plasma with a smooth initial density profile is lower than that of a sharp boundary [25]. So modification of the initial plasma density profile should be helpful to reduce ion energy. Pre-pulse is widely adopted to modify the initial density profile [26]. In our previous works [27, 28], we have demonstrated that ion energy from laser-produced Sn plasma could be significantly reduced nearly without loss of in-band CE from laser to 13.5 nm EUV light by introducing a low energy pre-pulse. The pre-pulse produces a neutral pre-plume with a gentle density profile; the main pulse interacts with the pre-plume instead of the infinitely sharp solid target.

In this paper, we present efforts to apply the dual pulse irradiation technique to Sn mass-limited targets. Thin Sn coatings were investigated as mass-limited targets. We demonstrated that higher ion energy accompanying Sn mass-limited targets could be maintained under 100 eV. Using a 30-nm Sn film coated on a silicon wafer, nearly the same in-band CE was obtained as compared with that of a slab Sn target irradiated by a single laser pulse.

2. EXPERIMENTAL ARRANGEMENTS

Experiments were carried out at Laser Plasma and Laser-Matter Interaction Laboratory of the University of California, San Diego (UCSD). The experimental arrangement is illustrated in Fig. 1. Two lasers are employed in the present experiments. One is a picosecond (ps) Nd:YAG laser (EKSPLA SL335), which could output 1.064 and 0.532μm laser

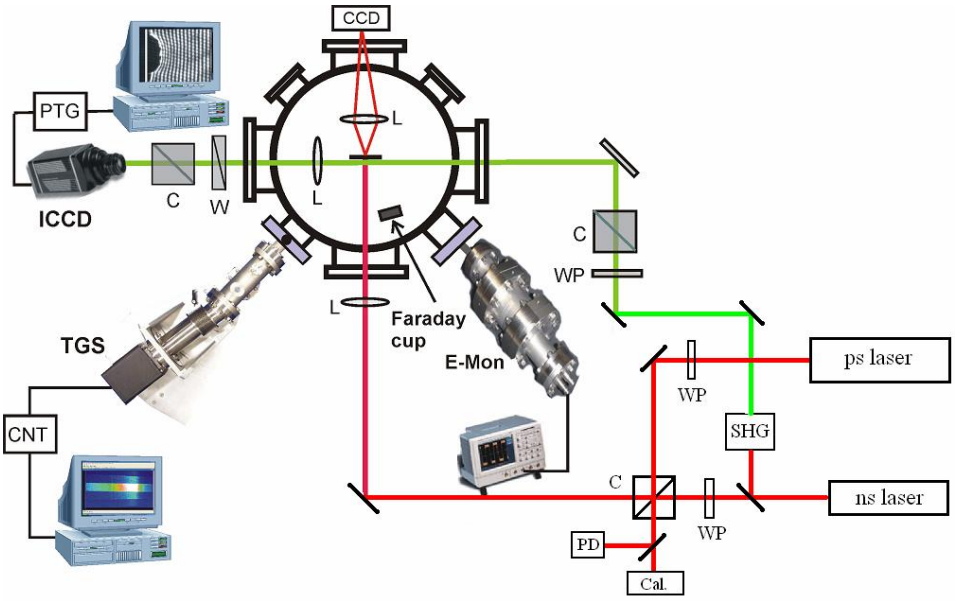

Fig. 1. Experimental arrangement for the generation of EUV light from plasmas irradiated by dual laser pulses. SHG-second harmonic generation, C-cube polarizer, WP-half wave plate, L-lens, PD-photodiode, Cal.-calorimeter, TGS-transmission grating spectrograph, ICCD-intensified CCD camera, W-Wollaston prism.

pulses with pulse durations from 130 to 550 ps. The other is a Q-switched Nd:YAG laser (Continuum Surelite II-10), which produces a 1.064 μm laser pulse with pulse duration of 7 nanoseconds (ns) and pulse energy of 650 mJ. The ps laser is used as pre-pulse to generate a pre-plume. The ns laser is used to heat the pre-plume to the optimum temperature for efficient 13.5 nm EUV light, called the main pulse hereafter. The two lasers are synchronized with a jitter less than 0.5 ns. The two laser beams are combined into a collinear path by a cube polarizer and focused by a same lens onto the target surface at normal incidence. The diameters of the focal spots and their overlapping are measured by an optical imaging method. The diameters of focal spots of the pre- and main pulses are 300 and 100 μm respectively.

Comprehensive diagnostics are employed to characterize the properties of EUV emission, debris emission, and the EUV plasma. In-band CE from laser to 13.5 nm EUV light is measured by an absolutely calibrated EUV energy monitor, E-Mon, from Jena Optik. The CE is integrated over a 2π solid angle. The spectrum of soft x-rays from the EUV plasma is observed by a transmission grating spectrograph (TGS) with a spectral resolution better than 1 nm. The E-Mon and the TGS are installed at opposite 45 degree angles with respect to the target normal in the plane of laser incidence. The ion energy spectrum is observed with a Faraday cup (FC) from Kimball Physics. The FC is biased with a –30 V voltage. The FC is placed inside the vacuum chamber at a distance of 15 cm from the plasma. Plasma density is observed using a time resolved Nomarski interferometer with a 532 nm probe beam [28]. The probe beam is split from the main pulse and converted into green light by a second harmonic generator (SHG), a type II KDP crystal. The density profile of the neutral plume generated by the pre-pulse is measured by shadowgraphy using a similar arrangement as the interferometer.

The dynamics of ions with low charge state and neutral particles are observed with spatially and temporally resolved visible light spectroscopy. The scheme of the spectroscopy is illustrated in Fig. 2. The plasma emission is imaged to the slit of a 0.5 m triple grating imaging spectrograph (Acton SpectroPro 500i). The plasma image is rotated 90 degrees by a pair of orthogonal Al mirrors, that is, the line of the laser incidence in horizontal plane is rotated to vertical plane. The dispersed spectra from different plasma regions located at various distances from the target surface in the line of laser incidence is recorded by a fast gated CCD camera (Princeton PIMAX) in a single shot. Time resolution better than 2 ns is achieved.

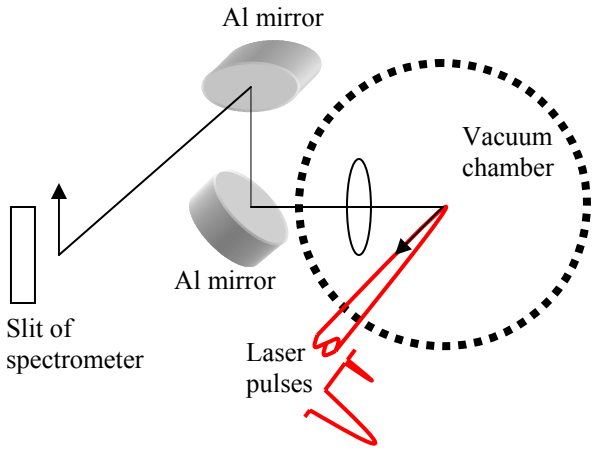

Fig.2. Schematic illustration of the spatially and temporally resolved spectroscopy

Several kinds of Sn targets, including high purity 1 mm thick Sn slab, 10 and 1 μm Sn foils, 100, 50, 30, and 20 nm Sn films coated over silicon wafers and plastic plates, are used in present experiments. Sn films are fabricated using an electron beam evaporator (Temescal BJD-1800); the thickness of the film is measured by a surface profiler (Ambios Technology XP-1) with a resolution better than 1 nm.

3. RESULTS AND DISCUSSIONS

3.1 Optimization of dual laser pulse irradiation technique

Efforts were carried out to reduce the necessary pre-pulse energy to achieve high reduction factor in ion energy. In previous works, the necessary pre-pulse energy to achieve 30 times reduction in ion energy was limited to 2 mJ. It is worth noting that the focal spot size of the pre-pulse is much larger than that of the pumping pulse in our experiments. The reason comes from the different divergent angles of the two laser beams. The pre-pulse laser has a smaller divergent angle as compared with that of the pumping pulse. So the foci of the two laser beams are located at different positions. In experiments, the target surface is always positioned near the focus of the main pulse, and the focus of the pre-pulse is located at a distance of 20 mm from the target surface. So a larger spot size results on the target surface for the pre-pulse.

In order to reduce the required pre-pulse energy, a beam compressor was inserted into the optical path of the main pulse to reduce its divergence. The beam compressor consists of a convex lens with a focal length of 40 cm and a concave lens with a focal length of 20 cm. The same divergent angle as the pre-pulse was obtained by adjusting the beam compressor. The images of the focal spots of the pre- and pumping pulses were measured by an imaging relay method. It is seen that the focal spot of the main pulse looks like an ellipse of 100×150 μm. The diameter of the focal spot of the pre-pulse is adjusted to 150 μm. As compared with the previous pre-pulse spot size, 300 μm, the required pre-pulse energy can be reduced by a factor larger than 4. The ion energy spectrum was observed using this beam compressor. It was found that more than 30 times reduction in ion energy could be achieved with a pre-pulse energy less than 1 mJ.

The effect of wavelength of the pre-pulse was investigated. Typical ion energy spectra obtained with an IR pre-pulse are shown in Fig. 3. It was found that more than 30 times reduction can be achieved using a IR pre-pulse with energy ~2 mJ. Compared with a green pre-pulse, an IR pre-pulse requires a higher energy to achieve 30 times reduction. Shadowgraphs of the pre-plume induced by the pre-pulses with green (0.532 μm) and IR (1.064 μm) wavelengths taken at delay time of 840 ns are shown in Fig. 4 (a) and (b) respectively. The pre-pulses have the same energy of 1 mJ. It is seen that the scale length of the pre-plume induced by the IR pre-pulse is smaller than that of a green pre-pulse. The difference between the green and IR wavelengths may come from laser absorption in the pre-plasma. The dominating absorption mechanism is inverse bremsstrahlung, which is inversely proportional to the wavelength of the laser pulse. More efficient absorption and ablation may result with a green pre-pulse, thereby requiring less energy.

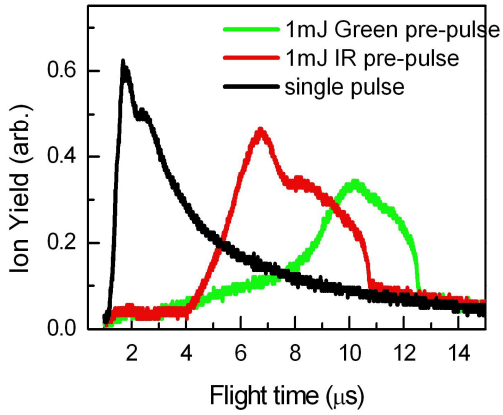

Fig. 3. TOFs from Sn plasma irradiated by dual laser pulses with a pre-pulse with wavelength of IR 1.064 and green 0.532 μm, and single pulse.

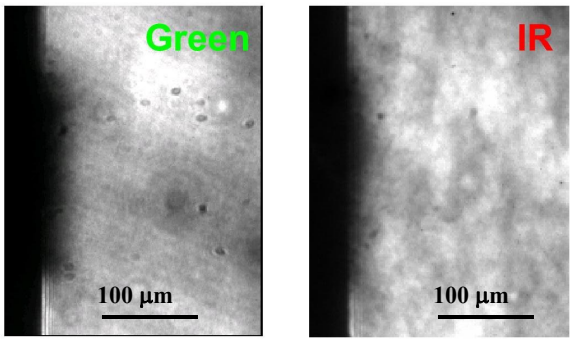

(a) (b)

Fig. 4. Shadowgraphs of pre-plume induced by the pre-pulse with wavelengths of (a) IR 1.064 and (b) green 0.532 μm respectively.

A typical spatially resolved spectrum of laser-produced Sn plasma obtained at intensity of 2×10^{11}W/cm^2 is shown in Fig.5. The lateral axis represents wavelength, and the longitudinal axis is distance from the target surface. The zero point on the longitude axis is the initial target surface. Neutral Sn atoms are visualized with the line at 452.4 nm due to the transition $5p^2$ 1S -5p6s 1P° of neutral Sn. Singly ionized Sn^{1+} is characterized with the lines at 533.2, 556.2, 558.9 and 579.9 nm due to the transitions of $5s^2$(1S)6p $2p^0$ 1/2-$5s^2$(1S)6d 2D 3/2, $5s^2$(1S)6p $2p^0$ 3/2-$5s^2$(1S)6d 2D 5/2, $5s^2$(1S)5d 2D 3/2-$5s^2$(1S)4f $2F^0$ 5/2 and $5s^2$(1S)5d 2D 5/2-$5s^2$(1S)4f $2F^0$ 7/2. It is seen that the energy of the neutral particle is much lower than that of ions even using a single pulse. The energy spectrum of the neutral particles is calculated from

the line intensity distribution along the spatial coordinate at 452.4 nm extracted from Fig.5. It is found that energy of the neutral particle is less than 100 eV. It is worth noting that only lines from ions with charge state 1+ can be identified due to the availability of atomic data [29]. It was found that other lines possibly from Sn ions with high charge states are much faster than those from neutral and Sn^{1+}. Note that the velocity of the particles depends on their ionization state. The spectra from neutral and Sn^{1+} observed with a dual-pulse are almost the same with that of single pulse. If the atomic data for ions with higher charge state is available, the dynamics of ions with various charger states higher than 1+ could be studied in detail with this spatially resolved spectroscopy.

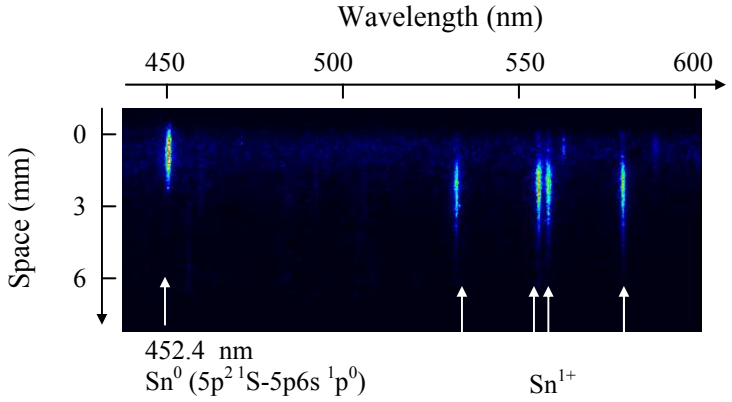

Fig.5. A typical spatially resolved spectrum of Sn

3.2 Properties of EUV and ion emission from thin Sn film targets

The soft x-ray spectrum from laser-produced Sn plasma was observed under the identical conditions as the ion spectrum measurement. Typical results with a slab (black solid line), 100 nm Sn film coated on a plastic plate (blue line), and 30 nm Sn film on a silicon wafer (red line) are shown in Fig.6. The laser intensity is 2×10^{11} W/cm^2. It is seen that the Sn film coated on plastic shows a much lower intensity around the wavelength of 13.5 nm as compared with those of a slab or film coated on a silicon wafer. The reason may come from the low density of Sn due to the mixing of Sn with C, H, and O atoms during evaporation. Lines at 12.9 and 15.0 nm are seen in Fig. 6. These lines are identified as the transitions $1s^22p$-$1s^24d$ and $1s^22s$-$1s^23p$ of OV ions respectively. Lower in-band CE and higher ion velocity were observed using Sn film coated on plastic as compared with those from Sn slab and Sn film coated on silicon wafer. A silicon wafer is always used in the following experiments.

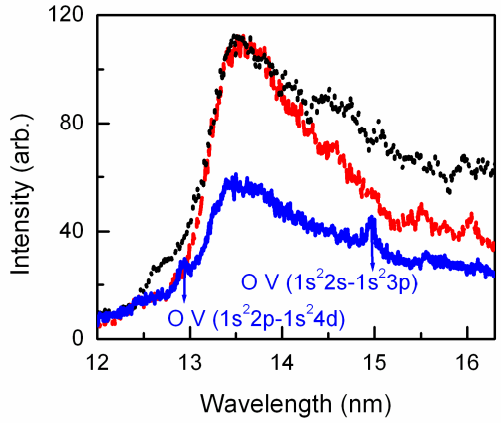

Fig.6. Soft x-ray spectra from Sn plasmas with 1 mm slab (black dot), 30 nm film coated on silicon wafer (red line), and 30 nm film coated on plastic plate (blue line).

Another notable feature in Fig. 6 is the narrower spectrum of the 30 nm Sn film on silicon as compared with that of a slab target. In-band EUV light centered at 13.5 nm comes from the unresolved transition array (UTA) of Sn^{8+} to Sn^{13+}. The width of the spectrum depends on the distribution of the charge state of Sn ions. Less Sn atoms are involved in mass-limited targets. So the change in charge states due to collisions is lower in mass-limited targets. A narrower spectrum results. This purification of the spectrum is helpful to reduce thermal heating of the EUVL system. Spectral narrowing also has been observed using targets with low concentration of Sn [17, 18].

The in-band CE from laser to 13.5 nm EUV light from Sn targets with various thicknesses was observed under the identical conditions used in the spectral measurement. Typical results as a function of target thickness irradiated by a single (black square) and dual pulse (red dot) are shown in Fig.7. It is seen in Fig.7 that in the case of a single pulse 30 nm is thick enough to get almost the same in-band CE from laser to 13.5 nm EUV light as compared with that of a bulk slab. It is worth noting in Fig.7 that for the case of dual laser pulses, the measured in-band CEs are nearly the same as compared with that of a single pulse with various target thicknesses. In the case of mass-limited target, less atoms are involved in the EUV plasma; therefore, less EUV light should be generated. This reduction in generation could be compensated by less re-absorption of the in-band 13.5 nm EUV light induced by the EUV plasma. So almost the same in-band CE is obtained with a mass-limited target as compared with that of a massive target, such that high in-band conversion efficiency and much lower ion energy could be obtained simultaneously by the combination of a mass-limited target and double pulses.

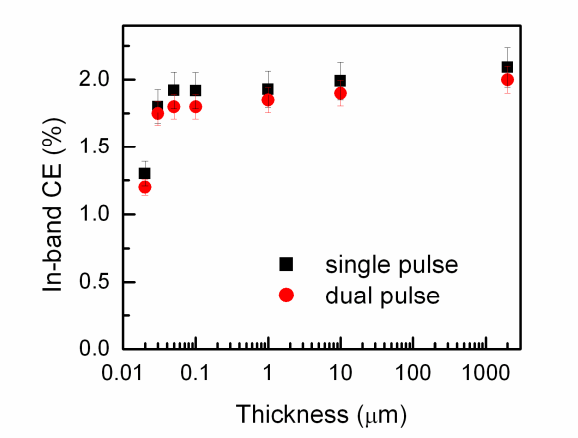

Fig.7. In-band conversion efficiency versus thickness of Sn target, red dot represents experimental data obtained with dual laser pulses, black square is from single pulse.

Time of flight of ions generated from laser-produced Sn plasmas was observed employing various Sn targets with thicknesses from 1 mm down to 20 nm. Typical results from a Sn film with a thickness of 30 nm and a slab target are shown in Fig. 8. The black dotted and blue dashed lines represent the results driven by a single pulse in vacuum and in ambient Ar gas with a pressure of 40 mTorr respectively; the green dashed and red solid lines are from dual laser pulses in vacuum and in 14 mTorr Ar respectively. The laser intensity of the pumping pulse is 2×10^{11} W/cm^2. The delay time between the pre- and the pumping pulses is 840 ns.

It is seen in Fig.8 that, in the case of a single laser pulse in vacuum, most ions are focused at early time and the flux peak is located around 1 μs. The corresponding kinetic energy of Sn ions located at the flux peak deduced from Fig. 1 is above 10 keV. This energy is higher than that of a massive Sn target driven by a single pulse (5 keV) [28]. This higher ion energy obtained with a mass-limited target coincides with Fujioka et al.'s measurement [21]. It was noted that this higher ion energy is always observed when the target thickness is less than 100 nm. The possible reason for the higher ion energy of the mass-limited target comes from the fact that less Sn atoms are involved in this plasma. Higher averaged charge state of Sn ions is obtained, and more kinetic energy can be gained during the plasma expansion.

However, it was noted that when dual laser pulses are used most ions are shifted to later time. As shown in Fig. 1, when a pre-pulse 840 ns prior to the pumping pulse is introduced, the flux peak is located later than 10 μs. Its corresponding kinetic energy is below 100 eV, which is comparable with that of a massive Sn target irradiated with dual laser pulses [28]. The reason for the reduction in ion energy in the case of dual laser pulses comes from the interaction of the pumping

laser pulse with the gentle density profile formed by the pre-pulse instead of the infinitely sharp boundary [28]. This shows that the dual-pulse irradiation technique could also be applicable to mass-limited targets.

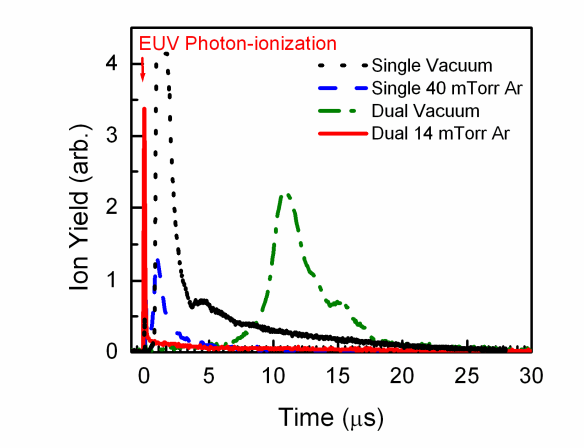

Fig.8. Soft x-ray spectra from Sn plasmas with 1 mm slab (black dot), 30 nm film coated on silicon wafer (red line), and 30 nm film coated on plastic plate (blue line).

Ambient gas or gas-puff has been considered as a standard technique to stop debris from the plasma in an EUV lithography system [30]. However, because of high absorption cross section of the gas at a wavelength of 13.5 nm, only very few kinds of gas, such as hydrogen, can be used in EUVL source system. Transmission of gas was calculated [31] and experimentally measured. Typical results of calculated and experimental measured in-band CE of Ar gas are shown in Fig. 9. The distance from the plasma to the photodiode of the E-mon is 70 cm. It is seen that the experimental measured value is even lower than that obtained from calculation. The possible reason comes the influence of the gas on the laser plasma interaction [32]. But further investigation is still necessary. Another issue relevant to the use of ambient gas is the ionization of the gas induced by the strong EUV light near the optics surface. The ionization yield depends on the pressure of the gas. So it is necessary to use inert gas and with a low pressure.

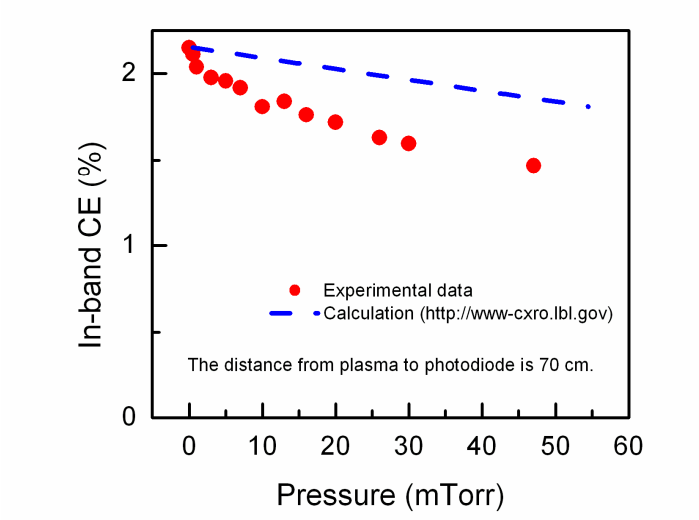

Fig.9. Calculated (blue dashed line) and experimentally measured (red dot) in-band conversion efficiency versus Ar gas pressures.

The stopping power of neutral gas can be simplified as [33],

$$S = kZ_1 Z_2^2 L / \beta^2 \qquad (1)$$

where $k = 0.3071/Z_2$ having units of keV/(mg/cm^2), Z_1 and Z_2 are the atomic numbers of target particle and ambient gas respectively, L is the stopping number, and $\beta = v/c$ is the relative velocity of target particles. Equation (1) predicts that gas is more efficient at stopping slow particles. It is seen in Fig. 8 that for a single pulse, even with 40 mTorr Ar, significant fast ions are still observed. However, in the case of dual pulses, ions could be nearly stopped with 14 mTorr Ar. The calculated transmission of Ar gas at 13.5 nm with pressures of 14 and 40 m Torr are 97 % and 88 % respectively with a distance of 70 cm. This shows that the use of dual pulses enables the use of inert Ar as the gas to stop ions in an EUVL system.

4. CONCLUSIONS

We demonstrated that high ion energy accompanying mass-limited Sn targets could be significantly reduced under 100 eV nearly without loss of CE by introducing a low energy pre-pulse. As thin as 30 nm Sn film could produce almost the same CE as compared with that of a slab target. The dual pulse irradiation technique enables the use of inert Ar gas instead of somewhat dangerous H. It was shown that the combination of dual laser pulses, magnetic field, mass-limited target, and ambient gas could substantially mitigate debris from Sn plasma.

5. ACKNOWLEDGEMENT

This work was supported in part by the von Liebig Center for Enterpreneurism and Technology Advancement, Jacob School of Engineering, University of California, San Diego. The authors would like to express thanks to Dr. S.S. Harilal for his help in experiments and invaluable discussions.

REFERENCES

1. Peter J. Silverman. “Extreme ultraviolet lithography: overview and development status”. Journal of Microlithography, Microfabrication, and Microsystems, 4, 011006 (2005).
2. See proceeding of the 5th International EUVL Symposium, 15-18 October 2006. Barcelona, Spain. https://www.sematech.org/7870/
3. Joseph Pankert, Rolf Apetz, Klaus Bergmann, Marcel Damen,Günther Derra, Oliver Franken, Maurice Janssen, Jeroen Jonkers, Jürgen Klein, Helmar Kraus, Thomas Krücken, Andreas List, Michael Loeken, Arnaud Mader, Christof Metzmacher, Willi Neff, Sven Probst, Ralph Prümmer, Oliver Rosier, Stefan Schwabe, Stefan Seiwert, Guido Siemons, Dominik Vaudrevange, Dirk Wagemann, Achim Weber, Peter Zink, Oliver Zitzen. “EUV sources for the alpha-tools”. Proc. SPIE 6151, 61510Q (2006)
4. Martin C. Richardson, Chiew-Seng Koay, Kazutoshi Takenoshita, C. Keyser, S. George, Somsak Teerawattansook, Moza M. Al-Rabban, and H. Scott. “Laser plasma EUVL sources: progress and challenges”. Proc. SPIE 5374, 447 (2004)
5. R. C. Spitzer, T. J. Orzechowski, D. W. Phillion, R. L. Kauffman, and C. Cerjana, J.Appl.Phys. 79, 2251 (1996)
6. Shinsuke Fujioka, Hiroaki Nishimura, Katsunobu Nishihara, Akira Sasaki, Atsushi Sunahara, Tomoharu Okuno,Nobuyoshi Ueda, Tsuyoshi Ando, Yezheng Tao, Yoshinori Shimada, Kazuhisa Hashimoto, Michiteru Yamaura, Keisuke Shigemori, Mitsuo Nakai, Keiji Nagai, Takayoshi Norimatsu, Takeshi Nishikawa, Noriaki Miyanaga,Yasukazu Izawa, and Kunioki Mima. “Opacity Effect on Extreme Ultraviolet Radiation from Laser-Produced Tin Plasmas”. Phys.Rev.Lett. 95, 235004 (2005).
7. Y.Tao, M.Nakai, H.Nishimura, S.Fujioka, T.Okuno, T.Fujiwara, N.Ueda, N.Miyanaga, and Y.Izawa. “A temporally-resolved Schwarzschild microscope for characterization of extreme ultraviolet in laser-produced plasmas”. Rev.Sci.Instrum. 75, 5173 (2004).
8. Y.Tao, H.Nishimura, S.Fujioka. A.Sunahara, M.Nakai, T.Okuno, N.Ueda, K.Nishihara, N. Miyanaga, and Y. Izawa. “Characterization of electron density profile of laser-produced Sn plasma for 13.5nm extreme ultraviolet source”. Appl.Phys.Lett., 86, 201501 (2005).
9. Y. Shimada, H. Nishimura, M. Nakai, K. Hashimoto, M. Yamaura, Y. Tao, K. Shigemori, T. Okuno, K. Nishihara , T. Kawamura , A. Sunahara , S. Fujioka, S. Uchida, N. Miyanaga, Y. Izawa and C. Yamanaka. Characterization of EUV emission from laser produced spherical tin plasma generated with multiple laser beams. Appl.Phys.Lett. 86, 051501(2005).

10. Björn A. M. Hansson, Igor V. Fomenkov, Norbert R. Böwering, Alex I. Ershov, William N. Partlo, David W. Myers, Oleh V. Khodykin, Alexander N. Bykanov, Curtis L. Rettig, Jerzy R. Hoffman, Ernesto Vargas L, Rod D. Simmons, Juan A. Chavez, William F. Marx, and David C. Brandt. "LPP EUV source development for HVM". Proc. SPIE 6151, 61510R (2006).
11. Chiew-Seng Koay, Simi George, Kazutoshi Takenoshita, Robert Bernath, Etsuo Fujiwara, Martin Richardson, and Vivek Bakshi. "High conversion efficiency microscopic tin-doped droplet target laser-plasma source for EUVL". Proc. SPIE 5751, 279 (2005).
12. Y. Tao, S. Farshad, H. Nishimura, R. Matsui, T. Hibino, T. Okuno, S. Fujioka, K. Nagai, T. Norimatsu, K. Nishihara, N. Miyanaga, and Y. Izawa, A.Sunahara and T.Kawamura. "Monochromatic imaging and angular distribution measurements of extreme ultraviolet light from laser-produced Sn and SnO2 plasmas". Appl.Phys.Lett. 85, 1919(2004).
13. Y. Tao, H.Nishimura, S.Fujioka, T.Okuno, N.Ueda, M.Nakai, K. Nagai, T.Norimatsu, K.Nishihara, N. Miyanaga, and Y. Izawa. "Dynamic imaging of extreme ultraviolet emission in laser-produced Sn plasmas". Appl.Phys.Lett. 87, 241502 (2005).
14. M. Lysaght, D. Kilbane, N. Murphy, A. Cummings, P. Dunne, and G. O'Sullivan. "Opacity of neutral and low ion stages of Sn at the wavelength 13.5 nm used in extreme-ultraviolet lithography". Phys. Rev. A 72, 014502 (2005)
15. M. C. Richardson, C-S. Koay, K. Takenoshita, C. Keyser, "High conversion efficiency tin material laser plasma source for EUVL," J. Vac. Sci. Technol. B, 22, 2, 785-790, (2004).
16. Takeshi Higashiguchi, Naoto Dojyo, Masaya Hamada, Wataru Sasaki, and Shoichi Kubodera. "Low-debris, efficient laser-produced plasma extreme ultraviolet source by use of a regenerative liquid microjet target containing tin dioxide (SnO2) nanoparticles". Appl. Phys. Lett. 88, 201503 (2006)
17. Keiji Nagai, QinCui Gu, ZhongZe Gu, Tomoharu Okuno, Shinsuke Fujioka, Hiroaki Nishimura, YeZheng Tao, Yuzuri Yasuda, Mitsuo Nakai, Takayoshi Norimatsu, Yoshinori Shimada, Michiteru Yamaura, Hidetsugu Yoshida, Masahiro Nakatsuka, Noriaki Miyanaga, Katsunobu Nishihara, and Yasukazu Izawa. "Angular distribution control of extreme ultraviolet radiation from laser-produced plasma by manipulating the nanostructure of low-density SnO2 targets". Appl. Phys. Lett. 88, 094102 (2006).
18. S. S. Harilal, M. S. Tillack, Y. Tao, B. O'Shay, R. Paguio and A. Nikroo. "Extreme ultraviolet spectral purity and magnetic ion debris mitigation with low density tin targets". Optics Letters, 31, 1549 (2006).
19. David C. Brandt, Igor V. Fomenkov, Norbert R. Böwering, Alex I. Ershov, William N. Partlo, David W. Myers, OlehV. Khodykin, Alexander N. Bykanov, JerzyR. Hoffman, Ernesto L. Vargas, Juan Chavez, Rodney Simmons, GeorgiyO. Vaschenko." LPP EUV Source Development for HVM". EUVL Symposium, Barcelona Spain, October 17 2006.
20. P. A. C. Jansson, B. A. M. Hansson, O. Hemberg, M. Otendal, A. Holmberg, J. de Groot, and H. M. Hertz. "Liquid-tin-jet laser-plasma extreme ultraviolet generation". Appl. Phys. Lett. 84, 2256 (2004)
21. Shinsuke Fujioka, Hiroaki Nishimura, Katsunobu Nishihara, Masakatsu Murakami, Youngces-G Kang, Qincui Gu, Keiji Nagai, Takayoshi Norimatsu, Noriaki Miyanaga, Yasukazu Izawa, Kunioki Mima, Yoshinori Shimada, Atsushi Sunahara, and Hiroyuki Furukawa. Properties of ion debris emitted from laser-produced mass-limited tin plasmas for extreme ultraviolet light source applications. Appl.Phys.Lett. 87, 241503 (2005).
22. Shinsuke Fujioka, Hiroaki Nishimura, Tsuyoshi Ando, Nobuyoshi Ueda, Shinichi Namba, Tatsuya Aota, Masakatsu Murakami, Katsunobu Nishihara, Young -G. Kang, Atsushi, Sunahara, Hiroyuki Furukawa, Yoshinori Shimada, Kazuhisa Hashimoto, Michiteru, Yamaura, Yuzuri Yasuda, Keiji Nagai, Takayoshi Norimatsu, Noriaki Miyanag,Yasukazu Izawa, and Kunioki Mima. "Energy spectra and charge states of debris emitted from laser-produced minimum mass tin plasmas". Proc. SPIE 6151, 61513V (2006)
23. Jean P. Allain, Ahmed Hassanein, Martin Nieto, Vladimir Titov, Perry Plotkin, Edward Hinson, Bryan J. Rice, R. Bristol, Daniel Rokusek, Wayne Lytle, Brent J. Heuser, Monica M. C. Allain, Hyunsu Ju, and Christopher Chrobak, Proc. SPIE 5751, 1110 (2005).
24. P. Mora. "Plasma Expansion into a Vacuum". Phys. Rev. Lett. 90, 185002 (2003).
25. Grismayer and P. Mora, "Influence of a finite initial ion density gradient on plasma expansion into a vacuum". Phys. Plasmas 13, 032103 (2006).
26. R. Kodama, T. Mochizuki, K. A. Tanaka, and C. Yamanaka, Appl. Phys. Lett. 50, 720 (1987).
27. Y. Tao, and M.S.Tillack. "Mitigation of fast ions from laser-produced Sn plasma for an extreme ultraviolet lithography source". Appl.Phys.Lett., 89,111501(2006).

28. Y. Tao, M.S.Tillack, S.S.Harilal, K.L.Sequoia, and F.Najmabadi. “Investigations on interaction of a laser pulse with a pre-formed Gaussian Sn plume for an extreme ultraviolet lithography source”. J. Appl. Phys., 101, 023305 (2007).
29. http://www.physics.nist.gov/
30. S.S.Harilal, B. O'Shay, Y. Tao, and M.S.Tillack. “Ion debris mitigation from tin plasma using ambient gas, magnetic fielda nnd combined effects. Sn plume for an extreme ultraviolet lithography source”. Appl. Phys.B, (in press)
31. http://www-cxro.lbl.gov/optical_constants/
32. Y.Tao, M.S.Tillack, S.S.Harilal, K.L.Sequoia, B.O'Shay, and F.Najmabadi. “Effect of shockwave-induced density jump on laser plasma interactions in low-pressure ambient air”. J.Phys.D:Appl.Phys. 39,4027 (2006).
33. J. F. Ziegler, “Stopping of energetic light ions in elemental matter”. J. Appl. Phys. 85, 1249 (1999).